Accurate CSI Estimation to Eliminate Unnecessary Transmission for MU-MIMO Networks

Shiyuan Zhang, Wei Xi, Qigui Xu, Kun Zhao, Yuanhang Cai
Lab of Smart Sensing and Mobile Computing
Xi'an Jiaotong University, China
{shiyuanzhang932,weixi.cs,qiguixu,pandazhao1982,Yuanhangxjtu}@gmail.com

Abstract

In large scale networks with many concurrently active IoT devices, Multi-user MIMO (MU-MIMO) is an important technology to improve data transmission efficiency, due to its ability of enabling multiple clients' concurrent transmissions. To achieve concurrent diversity gains, the network resource allocation relies on the feedback of Channel State Information (CSI) from clients. Inaccurate CSI estimation and unnecessary CSI feedback, however, heavily degrade the capacity and throughput of a MU-MIMO network, leading to superfluous energy consumption and potential channel collision of battery constrained wireless systems (EWS) in IoT.

Pursuing smart CSI feedback, we present QUICK, a protocol to achieve CSI quality estimation and power reallocation based on self-adaptive beamforming before data transmission, which could improve the CSI quality and reduce bit error rate (BER) efficiently. Based on the accurate CSI estimation, QUICK introduces a mobility-aware mechanism to eliminate unnecessary CSI feedback within coherence time. QUICK is fully compatible with the current IEEE 802.11ac standard and most state-of-the-art CSI feedback strategies, and is easy to be deployed on existing WiFi systems. Our software-radio based implementation and testbed experimentation demonstrate that QUICK substantially improves the throughput of both MU-MIMO downlink and uplink by 100% to up to 5×.

Categories and Subject Descriptors

C.2.1 [**Computer-Communication Networks**]: Netowrk protocol—*Network architectures;*

General Terms

Design, Experimentation, Performance

Keywords

MU-MIMO Networks, CSI quality estimation, Embedded wireless systems

1 Introduction

Advancements in computing and networking gave birth to the Internet of Things (IoT), which plays an increasingly indispensable role in modern life. Efficient access to the network is necessary, especially when transmitting data in large scale networks with many concurrently active IoT devices. Fortunately, the Multi-user MIMO (MU-MIMO) technology in IEEE 802.11ac standard holds the potential to substantially improve spectrum efficiency, by allowing concurrent transmissions between a multi-antenna access point (AP) and multiple users. In MU-MIMO, users need to report the estimation of its Channel State Information (CSI) to AP, and the AP selects the concurrent users with strong channel orthogonality to maximize total capacity.

Energy consumption must be taken into consideration when utilizing battery constrained embedded wireless systems (EWS) in MU-MIMO networks. With new chipsets becoming available, it is feasible to use WiFi enabled battery powered nodes in the IoT. For example, Bor et al.[3] have analyzed the energy consumption patterns of WiFi enabled nodes and have shown that future improved WiFi chips are likely to support common sensing and actuation tasks. However, there is still superfluous energy consumption that shortens the lifetime bound of battery powered EWS significantly in MU-MIMO networks, which mainly comes from invalid data transmissions, retransmission and unnecessary CSI feedback.

Invalid data transmission which mainly stems from inaccurate CSI estimation, is a major cause of the degraded performance in MU-MIMO network. CSI estimation is the fundamental requirement for various versions of MU-MIMO, *e.g.*, precoding & successive interference cancellation [9], rate adaptation [7], channel control [21], and some specific MU-MIMO applications [1, 11, 27]. Most recent research assumes perfect CSI in MU-MIMO networks, which is not true in many practical applications. In fact, inaccurate CSI estimation is usual in real-world MU-MIMO transmission due to noise. Based on our empirical study shown in section 3, if one user reports inaccurate CSI, its own downlink performance will become poor. Even worse, the uplink transmission of all the concurrent users may be incorrectly decoded by the AP. Under this situation, MU-MIMO transmission becomes extremely inefficient. Traditional error recovery methods such as data retransmission cannot resolve this problem effectively, which leads to superfluous energy con-

International Conference on Embedded Wireless Systems and Networks (EWSN) 2019
25–27 February, Beijing, China

ISBN: 978-0-9949886-3-8

sumption and channel collision. Unfortunately most existing solutions that aim to improve MU-MIMO throughput only focus on data recovery and ignore the CSI quality.

Unnecessary CSI feedbacks [22] in MU-MIMO network is another major cause which leads to low network throughput and superfluous energy consumption. When the user population is large, the channel resource spent on CSI feedback will overwhelm that spent on data transmission. Prior solutions for reducing this overhead mainly focused on feedback compressing or distributed user selection [29]. Unfortunately, those approaches only take effects after proper transmission modes and user groups are selected, which are impractical for uplink in MU-MIMO [15]. Some studies, *e.g.*, OPUS [28], reduce CSI overhead via AP's iterative probing. In each round, it enables a distributed contention mechanism that each user evaluates its orthogonality with the selected users. Then, the best user is distributed selected to join the current group. Only the selected users feedback their CSI. When the user population grows, these solutions are ineffective because collisions may frequently happen, which will result in system performance sliding down.

In this paper we propose to "prevention in advance" before data transmission to eliminate all the unnecessary transmission including both inaccurate CSI feedback and data transmission. We argue that efficient channel quality estimation and power reallocation before data transmission is a crucial issue in improving MU-MIMO performance, which is also a challenging task. Based on that CSI can be utilized to sense the mobility of wireless devices (For example, Bagci et al. [2] used CSI information to deduce device mobility for security purposes), we use CSI to estimate the moving speed of wireless devices, and eliminate unnecessary CSI feedback based on the devices moving speed.

In this paper we present QUICK, a protocol that allows users to assess CSI-quality, improve CSI accuracy, and reduce CSI feedback. QUICK works in three phases. 1) QUICK evaluates CSI-quality based on the distribution of received training symbols in the VHT preamble of the null data packet (NDP). 2) QUICK uses downlink beamforming to improve the SNR to obtain high-quality CSI. 3) QUICK allows users to reply with lightweight ACK instead of a long CSI packet, if the previously CSI is still valid for subsequent MU-MIMO data transmission.

We summarize our contributions as follows.

1. We use both theoretical and experimental results to show that inaccurate CSI feedback is one root cause to hurt MU-MIMO performance. This is the first work to target on real-time CSI-quality assessment and fast improvement which provides accurate CSI for IoT application to reduce superfluous energy consumption and channel collision.

2. We propose a device moving speed estimation method using only CSI, and develop an adaptive CSI feedback algorithm according to the motion state which is relevant to coherence time. QUICK eliminates unnecessary CSI feedbacks by replying a lightweight ACK frame to reuse historical CSI within coherence time. The system throughput can be further improved, and superfluous energy consumption caused by unnecessary CSI feedback could be reduced.

3. We conduct extensive real-world experiments under practical settings, with prototype implementation using software-radio devices. Results show that QUICK significantly improves the throughput of both uplink and downlink of MU-MIMO.

2 Related Work

Multiple-User MIMO (MU-MIMO)[8] [17], exploiting multiple antennas to send packets simultaneously to different recipients in order to increase the throughput further. Both the 802.11n and 802.11ac protocols use the technology of Beam Forming (BF) [23] to improve the SNR by concentrating the transmitted energy on the target receiver. In addition, channel state information (CSI) [25] [10] is introduced in the MU-MIMO network to resist the effects of multipath effects and frequency selective fading, and accurately predict the Packet Delivery Ratio (PDR) so as to select the best transmission strategy. The CSI is usually fed back to the wireless access point (AP) by the mobile device. The AP precodes the user data according to the CSI to eliminate interference between users. Therefore, timely and accurate CSI is very essential for the wireless network. CSI feedback reduction methods mainly fall into two categories: CSI feedback compression or distributed user selection. Nowadays, different compression methods are available to reduce the volume of CSI matrix. The CSI-SF method [5] uses the CSI value of a single data stream to predict the CSI value of multiple data streams, thereby reducing the oversampling of the CSI. The AFC method [29] adaptively selects the compression level of the CSI based on the decrease of the SNR caused by the compression of noise. However, such methods neither distinguish whether the mobile device is stationary or moving, nor know whether it needs to feedback CSI in a certain communication, which cannot reduce the number of CSI feedbacks. OPUS [28] reduces CSI overhead via AP's iterative probing. Signpost [33] achieves scalable MU-MIMO signaling with zero CSI feedback. In addition, Gabriel [4] reuses CSI by checking its validity period, which is obtained by F test of two CSI.

As for the methods of device motion detection, there are also two categories: Sensors based and physical layer information of wireless infrastructures based methods. Some sensors, such as accelerometers, GPS, gyroscopes, etc., used to provide the relatively accurate motion information (motion acceleration, rotation direction, physical location, etc.) of the device [19]. Besides, existing wireless infrastructures enable various kinds of IoT applications. For example, Smokey [31] achieves a ubiquitous smoking detection with commercial WiFi infrastructures, and Zheng et al.[32] elaborates on the design and implementation of such system based on Channel State Information in WiFi. Some physical layer information of the communication system can also be used to detect the physical location or direction of motion of the device [24, 26], which is applicable in 802.11ac without relying on specific hardware. Shangguan et al. [20] propose the phase profiling approach to relative localization of RFID tags by exploiting the spatial temporal dynamics in tag phase profiles. CSI similarity can be used [14] to detect device motion and environmental changes and reflects the profiling of the fine-grained multipath between the client and the AP, based

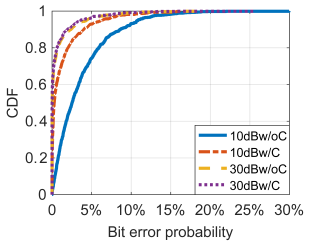

Figure 1. The impacts of imperfect CSI in uplink case

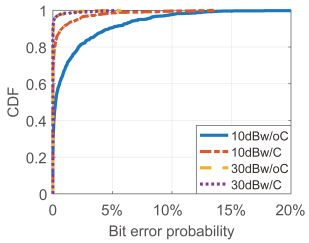

Figure 2. The impacts of imperfect CSI in downlink case

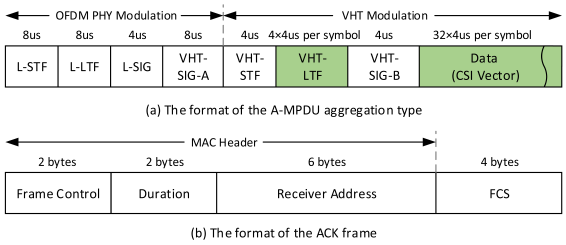

Figure 3. CSI feedback overhead analysis

on the channel states of adjacent data packets. However, it is difficult to distinguish the rotation of the device and the direction of motion only by CSI similarity. RoFi [16] senses the rotation of device using Power Delay Profile (PDP) similarity and achieves rotation-aware CSI feedback.

3 Impact of CSI

Through experimental results, we will show that inaccurate CSI estimation of a user will cause significant performance downgrading of both downlink and uplink in MU-MIMO. We make a conclusion that it is essential to ensure that every user participating MU-MIMO provides an accurate CSI estimation.

Figure 1 demonstrates the impacts of imperfect CSI on bit error probability (BEP) in uplink case. We use 256-QAM modulation and evaluate the BEP in different SNR cases (10dB and 30dB). We can see that in high SNR case (30dB), both the BEPs with and without CSI calibration (30dBw/C and 30dBw/oC, we will detail the CSI calibration technique in subsequent sections) would reach mean values of 0.0053 and 0.0058, respectively. The CSI calibration will improve about 8% PER. However, in low SNR case (10dB), the importance of CSI calibration becomes evident. We can see the mean BEP without calibration would rise to 0.039 while the one with CSI calibration would maintain 0.012. In other words, the CSI calibration operation would make the BEP drop to $1/3$ of the original one.

In downlink case, since precoding operation is processed before communication, the situation is slightly better than uplink case. Figure 2 demonstrates the impacts of imperfect CSI on bit error probability (BEP) in downlink case. In order to compare with uplink cases, we use the same modulation and SNR configuration to evaluate the performance. Under the same condition, the BEP in downlink cases is much better than that in uplink cases. In high SNR case (30dB), both the BEPs with and without CSI calibration would reach mean values of 0.0006 and 0.0007, respectively. In low SNR case (10dB), the importance of CSI calibration also becomes evident. We can see the mean BEP without calibration would be 0.0131 while the one with CSI calibration would maintain 0.0034 . In other words, the CSI calibration operation would make the BEP drop to $1/4$ of the original one in downlink case.

CSI reporting is time-consuming. Reporting a CSI vector by a user may take up to 180μs by sending a frame in Fig. 3(a). We propose that a user may simply reply an ACK to indicate no change of the CSI, which only costs 4μs as shown in Fig. 3(b). Hence our second goal in QUICK is to eliminate unnecessary CSI reports to improve channel efficiency.

4 QUICK Protocol Design

4.1 Work Flow of QUICK

QUICK is completely compatible with 802.11ac standard and existing distributed user selection mechanism (*e.g.*, OPUS [28]), except that QUICK adds a fixed update operation on CSI Matrix List (CML). In QUICK, a CSI quality assessment method is first proposed to determine whether the current CSI is qualified for data transmission. Then, for those users with inaccurate CSI, a CSI quality improvement process is conducted. Finally, based on the accurate CSI, a CSI feedback reduction method based on device moving speed is proposed. Specifically, QUICK works as follows:

(**i**) First, the AP broadcasts the NUll Data Packet (NDP) frame including VHT Long Training Field (VHT-LTF) for MU-MIMO setup and measurement, same in 802.11ac.

(**ii**) Each user estimates the CSI according to received VHT-LTF, puts the CSI values into a data packet and then transmit the packet to AP. The data packet also includes VHT-LTF which can be used to estimate the CSI again by the AP. Therefore, AP has two sets of CSI values. One is obtained from data field, the other is estimated from the VHT-LTF in the preamble.

(**iii**) After receiving the CSI feedback, AP estimates the BER according to the distribution of symbols in constellation diagram to assess CSI quality.

(**iv**) The AP separates the CSI quality of users using a threshold value β. Users with low-quality CSI will undergo a CSI recovery process to improve the CSI accuracy.

(**v**) A user will only report its current CSI to the AP when the channel coherence time of the last reused CSI is expired or its motion state changes. Otherwise, the user only needs to feedback lightweight ACK instead.

4.2 CSI-quality Assessment

We first introduce how the AP can assess the CSI-quality of different users and select those with inaccurate CSI to improve their accuracy. As is defined in many existing works[23], CSI quality is the accuracy of CSI for AP to precode/decode the data packets. In QUICK, for *every user*, we calculate the variance of distances between symbol coordinates and their corresponding symbol points in the constellation diagram, and use these distances to infer the BER. The

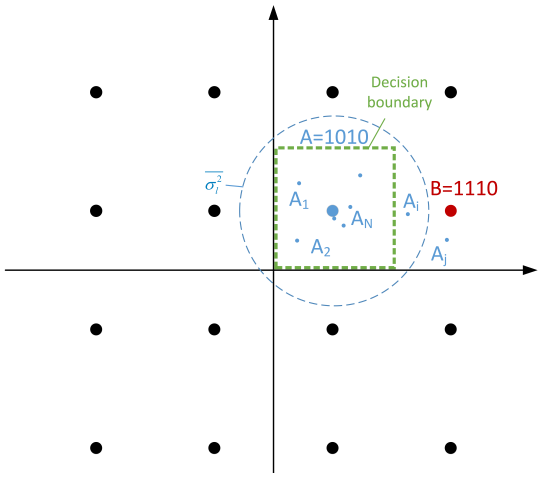

Figure 4. CSI Mapping in constellation diagram with 16QAM modulation

idea is shown in Fig. 4. The received symbol coordinates in 16QAM may be deviated from the actual symbol points such as A_1 to A_N. If the distance is much larger and the symbol point is outside of the *decision boundary* of A in the constellation diagram, such as A_j, this symbol will be recovered to a wrong one such as B. Hence the probability of the symbol points outside of the decision boundary among all test cases can infer the channel qualify and CSI accuracy of the user. In this way, we can estimate the CSI quality with two universally admitted reasonable assumptions [23, 27]:

A1: The CSI is invariant for several successive packets within a coherence time.

A2: The noise follows Gaussian distribution as mentioned in Section 3, *i.e.*, $n \sim \mathcal{CN}(0, \sigma^2)$.

Note the decision boundary cannot be easily obtained, we will calculate the decision boundary by first obtaining the upper bound of the deviation of the Gaussian noise at a user.

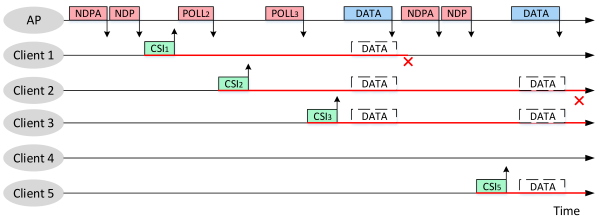

Figure 5. CSI feedback mechanism in QUICK.

After AP broadcasting training frame to each user l, the user l calculates its own CSI and replies to AP using collision avoidance, as shown in Fig. 5. Based on**A1**, we know that the replied data X is stable. Based on **A2**, we know AP can obtain replied data with noise n

$$Y_S = H_{X_l} X_l + n \tag{1}$$

where there are S AP antennas, *i.e.*, $Y_S = [y_1, \cdots y_i, \cdots, y_S]$, and H_{X_l} is the CSI vector of X_l. In quality assessment process, we should estimate the variance of noise n to decision the boundary.

Utilizing the preambles of feedback signal, AP can calculate the CSI $\widehat{H}$ as users have done and restore the transmitting signal $\widehat{X}$ according to 802.11ac standard. We can estimate the variance of noise σ^2, and the MU-MIMO SNR $\frac{||\widehat{H}||_F^2}{\sigma^2}$ where $||H||_F$ denotes the Frobenius norm of matrix H that includes the CSI vectors from all users. Define the scalar $\delta_{i,l} = 2\mathcal{R}(y_i H X_l) - (HX_l)^H (HX_l)$ where $\mathcal{R}(X)$ is the real part of X and H^H is the Hermitian matrix of H.

Leveraging maximum likelihood method, we have

$$\frac{\partial \mathcal{L}(y_i;\sigma^2)}{\partial(\sigma^2)} = -\frac{S}{\sigma^2} - \frac{y_i^H y_i}{\sigma^4} - \frac{\sum_{l=1}^{M} \frac{\delta_{i,l}}{\sigma^4} \exp\left(\frac{\delta_{i,l}}{\sigma^2}\right)}{\sum_{l=1}^{M} \exp\left(\frac{\delta_{i,l}}{\sigma^2}\right)} = 0$$

where $\mathcal{L}(\cdot)$ is the likelihood function.

Hence, if AP receives R symbols, we can estimate the upper bound of noise $\overline{\sigma^2}$ as follows (see detail in [6]),

$$\overline{\sigma^2} \approx \frac{1}{RS}\left(\sum_{i=1}^{R} y_i^H y_i - \sum_{i=1}^{R} \max(\delta_{i,l})\right)$$

We illustrate the noise bound in Fig. 4. The blue circle depicts the upper bound $\overline{\sigma^2}$. In general, with the increase of sample size R, the upper bound of noise variance would approach the ground truth, *i.e.*, $\overline{\sigma^2} \to \sigma_+^2$ from positive direction. In contrast, if the R is small, $\overline{\sigma^2}$ would much bigger than σ^2.

If the distance between restored symbol $\widehat{X}$ and the corresponding constellation point of X is less that than the decision boundary, the receiver can demodulate the symbol correctly, otherwise it would get a series of error bits. Based on Equation (1), we can get that for l-th-user, we have

$$D\left(\widehat{X}_l - X_l\right) = D\left(\frac{Y_l}{H_l} - X_l\right) = D\left(\frac{N_l}{H_l}\right) = \frac{\sigma_l^2}{\|H_l\|_F^2}$$

where $D\left(\widehat{X}_l - X_l\right)$ is the distance of the received symbol to the actual symbol point on the c-diagram and σ_l^2 is the variance of noise. That means the variance of distance is the reciprocal of l-th user's SNR $\frac{||H_l||_F^2}{\sigma_l^2}$.

With the distance variance, we can estimate the upper bound of the BER. Denote the decision distance as d_M (Note that different modulation method has different decision distance). According to Chebyshev's inequality, we can get

$$P\left(\left|\widehat{X}_l - X_l\right| \geq d_M\right) \leq \frac{D(\widehat{X}_l - X_l)}{d_M^2} = \frac{\sigma_l^2 \Big/ \|H_l\|_F^2}{d_M^2} \tag{2}$$

Since $\sigma_l^2 < \overline{\sigma_l^2}$, we can calculate the upper bound of $P\left(\left|\widehat{X}_l - X_l\right| \geq d_M\right)$ by substituting $\overline{\sigma_l^2}$ calculated from the maximum likelihood method.

QUICK sets a threshold β to decide whether it needs to start the CSI recovery process for this user. The Equation (2) infers that the probability of the misclassified symbol is upper bounded by $\frac{\overline{\sigma_l^2} \Big/ \|H_l\|_F^2}{d_M^2}$ under M-QAM modulation system.

Hence, if $\frac{\overline{\sigma_l^2}/\|H_l\|_F^2}{d_M^2} < \beta$, we can infer that the existing CSI is still qualified for communication and there is no need to start CSI recovery. Otherwise, QUICK should start the l-th user's CSI recovery process.

4.3 CSI-quality Improvement

For each user with inaccurate CSI, QUICK recovers its CSI by improving the value of Signal Noise Ratio (SNR). SNR can be estimated by Log Likelihood Ratio Calculation:

$$\mathrm{SNR} = \left(\frac{Q^{-1}(P_e)}{r_M}\right)^2 \tag{3}$$

where $Q^{-1}(P_e)$ and r_M are the inverse Q-function of bit error probability P_e and the coefficient corresponding to the modulation methods [13]. For the BPSK and QPSK modulations, r_M will be $r_{\mathrm{BPSK}} = \sqrt{2}$ and $r_{\mathrm{QPSK}} = 1$, respectively. From the derivation of Equation (3) in [18], we can see that P_e is the probability that error bits occur.

Since CSI estimation must be recovered within the coherence time, its recovery must be quick. QUICK utilizes *beamforming*, a preferred technical method applied in 802.11ac, to quickly enhance SNR to obtain accurate CSI from a user via preferentially direct its energy toward the selected receiver.

After reporting each user's CSI to AP, AP can obtain a list of users who need CSI recovery using the threshold β. Suppose the list includes T users $\Lambda = \{\Lambda_1, \cdots, \Lambda_{\mathfrak{T}}\}$ and $\overline{\sigma_{\Lambda_1}^2} < \overline{\sigma_{\Lambda_2}^2} < \cdots < \overline{\sigma_{\Lambda_{\mathfrak{T}}}^2}$. To guarantee accurate CSI by beamforming, for l-th user in Λ, the allocated power should be bigger than $\frac{\overline{\sigma_l^2}}{\beta d_M^2}$ to make the boundary crossing probability less than β. Let P be the total power the AP can allocate within a short period. If $P < \sum_{l\in\Lambda} \frac{\overline{\sigma_l^2}}{\beta d_M^2}$, i.e., the power is insufficient for all users that need CSI recovery, then we just do not include a few users with worse channel qualify until $P \geq \sum_{l\in\Lambda^+} \frac{\overline{\sigma_l^2}}{\beta d_M^2}$ for the largest set Λ^+.

Hence we can formalize this nonlinear optimization problem as follows

$$\arg\max_{\Delta p_l^{new}} \sum_{l\in\Lambda^+} \log\left(1 + \frac{\Delta p_l^{new} + \frac{\overline{\sigma_l^2}}{\beta d_M^2}}{\overline{\sigma_l^2}}\right)$$
$$s.t. \begin{cases} \Delta p_l^{new} \geq 0 \\ \sum_{l\in\Lambda^+} \Delta p_l^{new} \leq P - \sum_{l\in\Lambda^+} \frac{\overline{\sigma_l^2}}{\beta d_M^2} \end{cases}$$

where the objective function is to maximize the benefit of allocating more power Δp_l^{new} for each user l in addition to the basic power $\frac{\overline{\sigma_l^2}}{\beta d_M^2}$.

This optimization problem can be solved by waterfilling algorithm [30] and we can get the reallocated power

$$p_l^{new} = \left(\frac{\mu}{\|w_l\|^2} - 1\right)^+ + \frac{\overline{\sigma_l^2}}{\beta d_M^2}$$

where $(x)^+ = \max\{x, 0\}$ and the weight w_l and water level μ is chosen to satisfy

$$\begin{cases} \|w_l\|^2 = [H_l H_l^*]_{l,l} \\ \sum_{l\in\Lambda^+} \left(\mu - \|w_l\|^2\right)^+ = P - \sum_{l\in\Lambda^+} \frac{\overline{\sigma_l^2}}{\beta d_M^2} \end{cases}$$

where H_l^* denotes the conjugate transpose of H_l. If $C_p < C_p^{new}$, that means the reallocated power can improve the total capacity and QUICK can start CSI recovery process. Otherwise, it is not suitable for MU-MIMO mode.

4.4 CSI Feedback Reduction Based on Device Mobility

QUICK utilizes a CSI feedback reduction scheme based on device mobility. First, QUICK uses physical layer information to estimate the device moving speed. Then, the channel coherence time can be predicted according to the speed range. Finally, QUICK sets the maximum user service time by fairness control component and determines whether the CSI needs to be updated.

4.4.1 Channel Coherence Time under Different Device Moving Speed

Channel coherence time: CSI has a validity period, the data packets within this time period can be decoded by the same CSI without increasing the bit error rate, and we call the validity period the *channel coherence time*. Therefore, if the user performs multiple data transmissions within the validity period of the CSI, it is unnecessary to report the CSI to the AP before each transmission, and CSI needs to be updated only when the CSI gets expired.

Device under different motion states has different channel coherence time. Within the channel coherence time, the device does not need to feedback current CSI to AP, historical CSI could be reused and only an ACK could be sent instead.Next we empirically show that device under different moving speeds has different channel coherence time. Fig. 6 shows the channel coherence time for different moving speeds in a practical indoor environment. The user in a stationary state has a relatively longer coherence time exceeding 250ms. Even at a moving speed of $1m/s$, the coherence time is much larger than the maximum packet transmission time specified by the 802.11ac protocol. Only users with high mobile speeds need a faster CSI update frequency. It can be seen that the MU-MIMO network requires the user to include a large number of redundant operations in the behavior of feeding back CSI before each round of data transmission, and this overhead can be reduced by reusing the historical CSI and sending an ACK frame instead.

Note that Channel coherence time is determined both by the device's moving speed and environmental changes. Therefore, the estimated coherence time by considering only device moving speed only serves as a coarse-grained prediction on the stability of the channel state, while the posterior CSI quality assessment method will ultimately decide whether the CSI is valid within the coherence time and needs recovery.

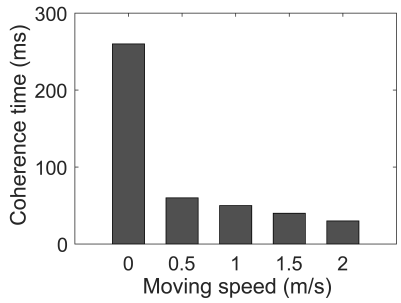

Figure 6. Channel coherence time under different device moving speeds.

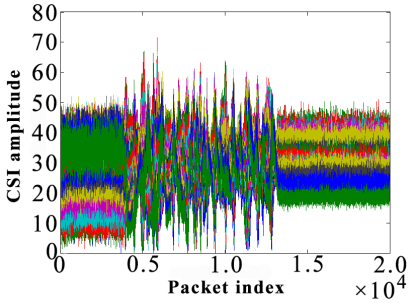

Figure 7. CSI amplitude variation.

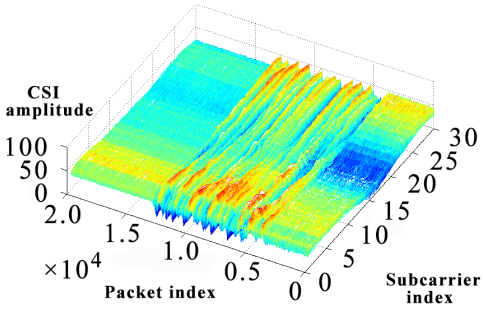

Figure 8. 3D CSI amplitude variation.

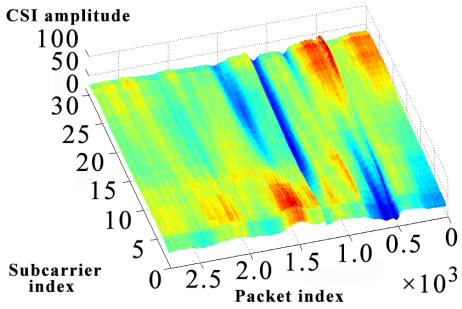

Figure 9. 3D CSI amplitude variation in another moving direction .

4.4.2 Estimating Device Moving Speed Using Physical Layer Information

In this section, we first reveal the fact that standing wave field exists in WiFi, and then elaborate on utilizing standing wave field to detect device moving speed.

The discovery of WiFi standing wave field: During experiments, by analyzing the channel state information CSI in the WiFi signal received by the signal receiver during the motion, it is found that the amplitude of the CSI shows a uniform stripe distribution. The original wave of the WiFi signal is interfering with its reflected wave or scattered waveform under the action of the indoor multipath effect, thereby generating a standing wave.

In order to quantify the influence of different dynamic behaviors of users on the signal, we designed the following experimental scene: In an empty room of about 30 square meters, a paper box with a height of about 80 cm was placed, where an AP is placed on the box, and there are no more items in the room. The experimenter user holds the signal receiving device (Receiver), keeps the hand posture unchanged, and advances at a constant speed in the direction of the AP. Receiver receives the WiFi signal sent by the AP and records it as the user moves. Among them, the AP always sends the WiFi signal continuously; User pauses for a period of time t1 after the start of the experiment, then moves linearly for a period of time t2, stops reaching after reaching a certain position, and then stops for a period of time t3; the Receiver keeps receiving the WiFi signal sent by the AP during the entire time period of the User (t1+t2+t3), and does not receive the signal before and after this time.

In order to analyze the detailed motion parameters of the User from the received WiFi signal, we extract the CSI in the WiFi signal, which can reflect the attributes of the signal during transmission. As can be seen from Fig. 7, receiver received nearly 2×10^4 WiFi packets as the User moves in which the amplitude of the CSI in the previous 0.4×10^4 WiFi packets is relatively stable, the amplitude values of about 0.9×10^4 CSI showed significant fluctuations, and the amplitude values of the last 0.7×10^4 CSI returned to a relatively stable state, with a ratio of 4:9:7. Since the User keeps moving at a constant speed during the motion, the ratio of the number of received data packets is the same as the ratio of the motion time. In the course of the experiment, t1:t2:t3=5:8:7, this ratio is basically the same as the ratio of the number of data packets in each period. Therefore, by analyzing this data, it is possible to obtain the duration of the different motion states during the movement.

In order to further analyze the detailed features of the user during the walking process reflected by the apparently fluctuating CSI amplitude value, the above data is displayed in a three-dimensional (3D) figure, as shown in Fig. 8. In the 3D map, the amplitude of the CSI shows a streak-like fluctuation, and the distribution of the fringes is relatively uniform. From the 30 subcarriers corresponding to the abscissa, the overall ripple exhibited by each subcarrier is very similar, which is related to OFDM technology. In fact, the center frequencies of the 30 subcarriers in the WiFi signal are relatively close, and they are distributed around the center frequency of the channel, so the overall ripples are very similar.

During the above experiment, however, user always moves along the line connected to the AP. When the direction of the linear motion is changed, that is, not along the linear motion connected to the AP, the CSI amplitude value

in the received WiFi signal is in another representation way, as shown in Fig. 9. Comparing Fig. 8 with Fig. 9, we suspect that the CSI in the WiFi signal has different performances in different directions of motion: When moving in the linear direction connected to the signal source, the obtained CSI has a uniform fringe distribution; while in other linear directions, the CSI stripe distribution is a little less obvious or even no streaked.

Combined with the physical definition and generating conditions of standing waves and the different directions of linear motion made during the experiment, it is known that since the original signal and the reflected signal transmitted by the WiFi signal source interfere with each other, a fixed standing wave field is formed on the signal transmission line, which contributes to the above phenomenon.

Nature of WiFi standing wave field: The WiFi standing wave is also a type of standing wave, except that the WiFi standing wave is formed by the WiFi signal. Therefore, the WiFi standing wave field combines the properties of both standing wave and WiFi signal.

In the standing wave, the point with the largest amplitude is called antinode, in which the amplitude is twice the amplitude of the original wave; the point with zero amplitude is called node; the distance between adjacent antinodes is:

$$x_{k+1} - x_k = (k+1)\frac{\lambda}{2} - k\frac{\lambda}{2} = \frac{\lambda}{2} \tag{4}$$

where x_{k+1} represents the $(k+1)$th antinode, while x_k represents the kth antinode.Similarly, the distance between adjacent nodes is:

$$x_{k+1} - x_k = [2(k+1)+1]\frac{\lambda}{2} - (2k+1)\frac{\lambda}{2} = \frac{\lambda}{2} \tag{5}$$

where x_{k+1} represents the $(k+1)$th node, while x_k represents the kth node. Moreover, according to the definition of standing wave wavelength, i.e., the distance between adjacent antinodes (or nodes) is the wavelength of standing wave, we can deduce that: The wavelength of the standing wave, formed by the interference between the original wave and the reflected wave of the WiFi signal, is half of the wavelength of the original signal (λ). This is why the interval between CSI stripes observed in the experiment is approximately equal.

The WiFi signals utilized in this article are based on the 802.11ac standard and can be selectively operated in the 2.4 GHz or 5 GHz band. When the 2.4 GHz band is selected, the wavelength of the WiFi signal is about 6 cm, so the WiFi standing wave wavelength at this time is about 3 cm. When the 5GHz band is selected, the wavelength of the WiFi signal is about 12 cm, so the WiFi standing wave wavelength is about 6 cm at this time. Consequently, as long as the number of standing wave periods in the received WiFi signal can be counted, the moving distance of Receiver on the line can be calculated, thus we can get moving speed.

Device speed estimation method: Some detailed studies of the device speed estimation based on WiFi signal have indicated that the distance between two adjacent antinodes (or nodes) towards any direction is half of the wavelength λ. When a device is moving indoor with a speed υ, a periodically ripple with a frequency f_c in CSI appears, i.e.,

$$f_c = 2\frac{\upsilon}{\lambda} \tag{6}$$

This relationship above tells us that the moving speed υ could be precisely estimated purely from CSI with the standing wave periods, i.e., $T_c = 1/f_c$. therefore, we can estimate the moving speed υ just by:

$$\upsilon = \frac{\lambda \times f_c}{2} \tag{7}$$

Here we basically illustrate the principle of standing wave field in WiFi. As for more detail, please refer to [12], a passive crowdsourcing CSI based indoor localization scheme including how to detect device moving speed.

4.4.3 Fairness Control Component

Since AP prefers to do user scheduling among users whose CSI is still usable in CML, the user with a longer CSI lifecycle based on channel coherence time would obtain a longer transmission time. Therefore, though the above proposed method has reduce CSI feedback overhead before data transmission as much as possible, the fairness for users to contend the channel will lead to serious throughput imbalance problems between different users. Especially, the channel coherent time of the user in the stationary scenario is much longer than that in the mobile scenario.

To solve this fairness problem, we set the maximum channel coherence time among all users in CML as a single time slice. Then, to make a tradeoff between user throughput fairness and network global throughput, every user would be served in a continuous time of as close as possible to this time slice for each scheduling, according to the formulation

$$T_l = \left[\frac{T_{\max}}{T_{c,l}} + \frac{1}{2}\right] \times T_{c,l}$$

Where T_l is the maximum continuous service time available to each user l, $T_{c,l}$ is the channel coherence time of the user at the current moment and $T_{\max}$ is the maximum channel coherence time in CML.

In addition, in order to ensure that users in the MU-MIMO network can be switched and scheduled frequently, the maximum single time slice $T_{\max}$ is set as 30 ms in this paper, which is also the average channel coherence time under the mobile scenario. Such service conditions will not affect the experience of users to use the Internet because every users will be scheduled efficiently.

5 Implementation and Evaluation

We conduct experiments using a QUICK prototype implemented by us and evaluate its performance.

5.1 Experimental Setup

We have implemented QUICK on USRP-N210 and USRP-X310 radio platforms with corresponding UHD software packages. An AP with multiple antennas is built with one USRP-X310 plus multiple SBX daughterboards. Each concurrent user is a USRP-N210 equipped with a SBX daughterboard, providing 40 MHz bandwidth. To allow multiple users to transmit concurrently, we connect the USRP-N210 devices to a laptop and control their transmissions by

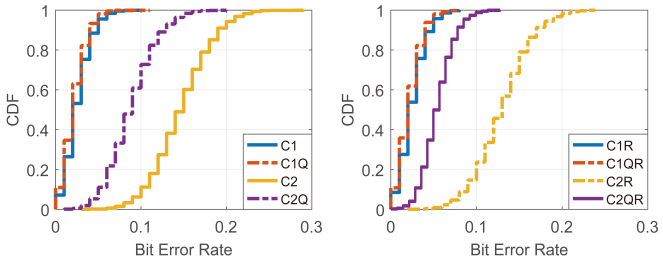

(a) Without data retrx (b) With data retrx

Figure 10. BER in downlink MU-MIMO

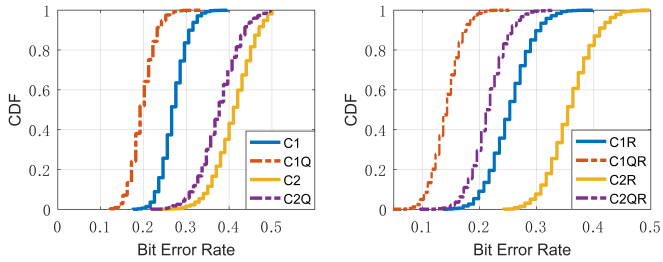

(a) Without data retrx (b) With data retrx

Figure 11. BER in uplink MU-MIMO

an instruction script. A similar instruction script is also installed in the two SBX daughterboards of USRP-X310.

For precise time synchronization, an external clock model USRP CLOCK DISTRIBUTION 782979-01 is adopted as a common clock source to connect the AP and users.

The entire system is compatible to the IEEE 802.11ac protocol standard and standard OFDM specifications, such as the modulations (16-QAM, 64-QAM, 256-QAM) and code rates. Hence, QUICK can be implemented on COTS NICs without hardware modification. For the user, it's supported by the NICs that the device could calculate the CSI upon receiving NDP from AP, and place the CSI into data field of a frame and feed the frame back to the AP. For the AP, constellation diagram is supported for NICs to decode received symbols. Given essential information, we could implement QUICK on the COTS NICs through programming its network card driver. Specifically, we simulate the different SNR conditions by tuning the transmission power within the range of [5dBm, 20dBm].

QUICK implements OFDM modulation, packet detection, channel estimation and symbol demodulation. Our CSI validation mechanism is added into channel estimation module. We use LabVIEW to achieve OFDM and the channel estimation.

5.2 BER Improvement under Low SNR

We first show if the BER can be improved using QUICK when a client is in bad situation and the SNR is low. This evaluates if the CSI can be recovered by QUICK. We allow two users $C1$ and $C2$ communicating with an AP with two antennas. We set SNR on $C1$ and $C2$ to be 10dB and 5dB, respectively. Neither of them are perfect but $C2$ is even worse. We illustrate and compare the BER with/without QUICK. For each test, we transmit 400 bits, and calculate the BER at each channel. We repeat our experiments 100 times for each scenario.

Fig. 10 illustrates the BER in downlink MU-MIMO. Fig. 10(a) depicts the cumulative distribution of BER without data retransmission. The mark Q means to use QUICK. We can see the BER of $C1$, the user with "OK" SNR (10 dB), is almost identical before and after QUICK, because there is no CSI recovery process for this user. Meanwhile, the user $C2$ with weak SNR can significantly reduce its BER by around 40% due to CSI calibration. Fig. 10(b) shows the BER improvement with data retransmission. Q and R denote CSI recovery and data retransmission, respectively. Similarly, there is no significant improvement on $C1$ because retransmission is not necessary. We can see that the curve $C2R$ is only slightly better than the curve of $C2$ and worse than that of $C2Q$ in Fig. 10(a), meaning retransmission does not help to improve BER a lot. The combined solution $C2QR$ performs significantly better by utilizing both CSI recovery and data retransmission: the average BER of $C2QR$ is only 5% and about 1/3 of that of $C2R$.

Fig. 11 shows the uplink BER under the same setup of Fig. 10. In Fig. 11(a), we can observe that both $C1$ and $C2$ experience BER reduction using QUICK. It is because the inaccurate CSI from $C2$ hurts the performance of $C1$. By improving the CSI accuracy of $C2$, both $C1$ and $C2$'s BER can reduce. As shown in Fig. 11(b), we find that simply applying retransmission does not help to reduce BER. However by combining QUICK and retransmission, the BER of both $C1$ and $C2$ can be improved to a very low level, by around 50% reduction.

5.3 Throughput Gain Using QUICK

Power reallocation is a crucial part of CSI calibration performance, thus we evaluated the effectiveness of CSI calibration instead, which is measured by the throughput gain of network in this section. We investigate the throughput gain of CSI recovery using QUICK in indoor environments and compare it with a state-of-the-art approach Smart[13].

Smart is a retransmission and rate adaptation method. It supports partial retransmissions before the FEC decoding and enables a combining-aware rate adaptation.

We generate a trace of packets, and then transmit the packets via the USRP platforms. In the experiments, we do not consider the channel contention since we mainly focus on improving CSI estimation and the entire network throughput. The number of users is equal to the number of the AP's antennas, which helps to avoid the collision caused by hidden terminals. Before concurrent transmission, each user estimates the CSI between the AP and itself by leveraging the training sequence transmitted from the AP.

We evaluate our QUICK protocol and Smart in both downlink and uplink for high and low SNR scenarios. We use two frame sizes, *i.e.*, 1000 bytes and 4000 bytes, to simulate both the short and long packet transmission in practice, denoted as "S" and "L" in Fig. 12.

Downlink scenario: Fig. 12(a) plots the cumulative distribution of the throughput in high SNR scenario for downlink using 1000-byte and 4000-byte packets. From the results, we see that QUICK brings evident better performance due to correct CSI estimations. In particular, the average

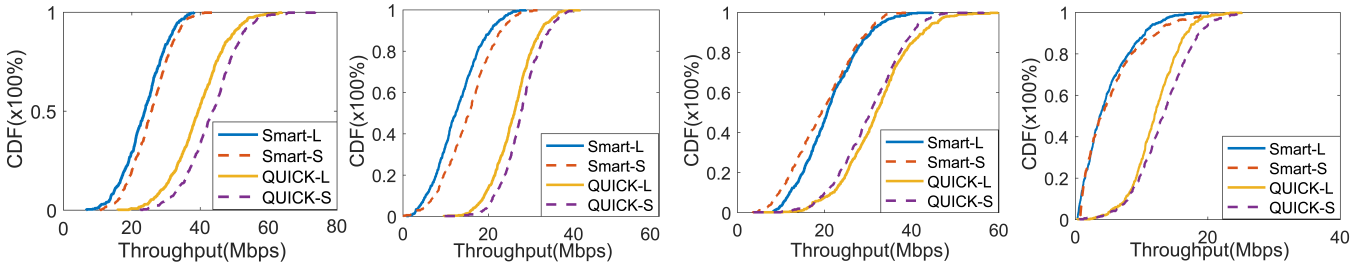

(a) High SNR in downlink (b) Low SNR in downlink (c) High SNR in uplink (d) Low SNR in uplink

Figure 12. The throughput estimation with different SNR in MU-MIMO

throughput gain of QUICK is about 90% compared to Smart with 1000-byte and 4000-byte packets. It is because that the CSI errors are not corrected in Smart, which raises a significant portion of failures in the precoding process. Unfortunately, the data retransmission mechanisms, used by Smart, cannot address these CSI errors well.

It is worth noting that QUICK performs better with a longer frame size. This is because a longer frame has a relatively smaller portion of preamble from the perspective of the entire packet. After performing QUICK, the BER corresponding to the parts of data in the packets is significantly reduced, which means longer packets can contain more correct bits than shorter packets with a same packet transmission rate.

In contrast, Smart has the similar throughput using 1000-byte and 4000-byte frames. Longer packet cannot increase throughput performance. Although long data packet can reduce the preamble proportion, the user cannot received the packet in downlink beamforming when the CSI is inaccurate.

In Fig. 12(b), we compare QUICK and Smart in low SNR scenario for downlink. QUICK still achieves much better performance. Specifically, QUICK increases the throughput gain by 100% compared to Smart. The throughput of QUICK and Smart becomes poor when using 4000-byte frames. The intuition behind is that a longer frame has a higher probability to experience bit transmission error with low SNR, which definitely increases BER and causing more rounds of data transmission.

Uplink scenario: Fig. 12(c) shows the cumulative distribution of throughput for QUICK and Smart in the high SNR scenario for uplink. QUICK still achieves 50% more throughput compared to Smart due to CSI estimation correction. Due to mutual interference of concurrent users, shorter data packets have more opportunities to be decoded correctly. The 1000-byte frame transmission has better performance than 4000-byte frame transmission.

In Fig. 12(d), we evaluate the performance in the low SNR scenario for uplink. As long as there is one user that provides low-quality CSI estimation, all concurrent transmitted data from other users may be decoded incorrectly, even if data retransmission is used. Smart has extremely poor throughput (mostly $<$10Mbps) in uplink MU-MIMO, when SNR is low. The improvement of using QUICK is hence significant: the throughput of QUICK is nearly three times of that of Smart in average.

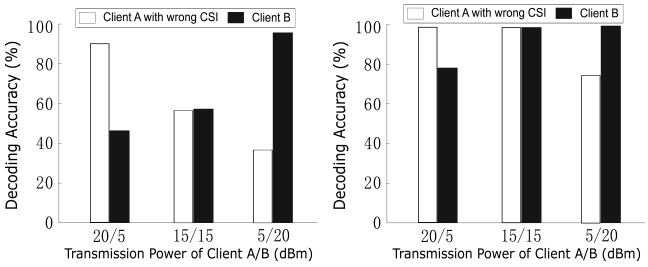

(a) Without QUICK (b) With QUICK

Figure 13. QUICK improvement for concurrent users

From the above, we can believe that the throughput gains of network using QUICK are better than Smart both in downlink and uplink, i.e., our proposed CSI calibration method is so significantly efficient that much unnecessary energy consumption and channel collision would be avoided in advance.

5.4 Interactions among Concurrent Users

Uplink MU-MIMO is extremely vulnerable to inaccurate CSI because inaccurate CSI from one user's transmission could corrupt those of other concurrent users. We conduct experiments to demonstrate how QUICK resolves this problem.

We let a client user, A, keep getting inaccurate CSI estimation. We set different values of SNR for A and another concurrent client user B. There are three possible cases: a) A transmits in high power (20dBm) and B transmits in low power (5dBm) (hence the SNR of A is high and that of B is low), b) both of A and B are transmitting in high power (15dBm), and c) A transmits in low power (5dBm) and B transmits in high power (20dBm) (hence the SNR of A is low and that of B is high).

The decoding accuracy of concurrent users without using QUICK is shown in Fig. 13(a). The experimental results show that when A transmits in 20dBm and B transmits in 5dBm, the decoding accuracy of A's signal is around 90% and the decoding accuracy of B's signal is very low $< 50\%$. When they both transmit in 15dBm, the decoding accuracy for both signals are low (around 50%). When A transmits in 5dBm and B transmits in 20dBm, decoding B's signal becomes better because A's influence is small.

Fig. 13(b) shows the decoding accuracy by using QUICK. QUICK can efficiently eliminate interactive interference among concurrent users. By recovering the CSI, AP will always have high decoding accuracy for the users with high

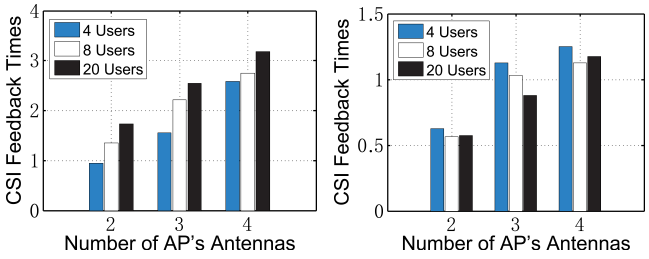

(a) Uplink MU-MIMO (b) Downlink MU-MIMO

Figure 14. The count of CSI feedback for continuous 100 rounds of transmission in QUICK.

SNR. In addition, AP also has improved decoding accuracy for the users with low SNR. QUICK provides a significant performance improvement from existing MU-MIMO transmissions.

5.5 CSI Feedback Reduction

In this section, we evaluated the effectiveness of reusing CSI within coherence time, which is based on estimated device moving speed. To illustrate this point, we first verify the performance of QUICK in reducing CSI feedback overhead. Fig. 14 (a) and (b) show the average number of CSI feedback times for continuous 100 rounds of uplink and downlink transmission in QUICK, respectively. Fig. 14 (a) shows that the average number of CSI feedback times in uplink increases with the growth of the number of users and AP's antennas. Obviously, feedback overhead can be significantly reduced by leveraging CSI reuse, as they only need less than 5 times of feedback for 100 rounds. When number of users reaches 20, the CSI feedback times is as close as the number of AP's antennas. Fig. 14 (b) shows that the average number of CSI feedback times in downlink is even smaller. It slightly increases while the number of AP's antenna increases. That means QUICK has a great performance in reducing CSI feedback for both uplink and downlink transmission, i.e., our proposed method to reuse CSI within coherence time, which is based on estimated device moving speed, turns out to be promising.

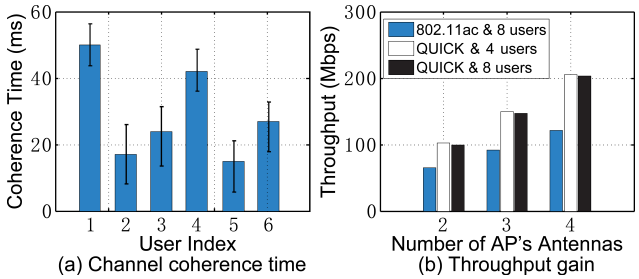

(a) Channel coherence time (b) Throughput gain

Figure 15. Throughput gain comes from CSI reusing.

Fig. 15(a) illustrates the channel coherence time of six concurrent users. We also examine the network throughput in Fig. 15(b). QUICK achieves 59.5% throughput gain over standard 802.11ac in a MU-MIMO network with a 4-antenna AP and eight users. We also observe that QUICK's throughput raises with the growing of AP's antennas. On the contrary, it decreases negligible while user population increases. The results show that with the CSI reduction mechanism, increasing the number of users will not hurt the overall throughput in MU-MIMO.

5.6 Compare Throughput under Accurate CSI

In this micro-benchmark, we compare the throughput of different MU-MIMO systems, and plot the results in Fig. 16(a)-(d). *Note that in this set of experiments all CSI reports are accurate. It is because the existing methods do not consider CSI accuracy. If we allow inaccurate CSI reports, the throughput of QUICK is much higher and existing methods are not comparable.*

For downlink MU-MIMO shown in Fig. 16(a) and (b) , Standard 802.11ac, OPUS and Signpost have almost identical throughput. Since there is no need of user selection, only concurrent users need to report their CSI. QUICK achieves the highest throughput among all schemes. The performance of QUICK in static scenario is better than it in mobile scenario due to longer coherence time. For uplink MU-MIMO shown in Fig. 16(c) and (d), OPUS [28], Signpost [33] and QUICK have too much higher throughput than 802.11ac. In order to select the orthogonal users, AP needs all the users to report their CSI in 802.11ac. OPUS, Signpost and QUICK achieve a distributed user selection which only need concurrent users to report their CSI.

5.7 Compare CSI Feedback Overhead

For CSI feedback overhead comparison, we compare QUICK with standard 802.11ac, OPUS and Signpost. Fig. 17(a) illustrates the CSI feedback overhead under different user population. We conduct these experiments with 4-antenna AP. While the overhead in standard 802.11ac and OPUS increases with the increase of total user number, the overhead in Signpost [33] and QUICK is almost constant. In a topology with 20 users, it achieves 6.3× , 7.9× and 1.3× overhead decrease over 802.11ac, OPUS and Signpost, respectively. Obviously, QUICK outperforms all other schemes. We run a benchmark scheme with 20 users to validate the effect of the number of AP's antenna on overhead, and plot the result in Fig. 17(b). It is clearly that the overhead increases when the number of AP's antenna grows in all these four MU-MIMO systems. However, the growth rate in QUICK is still in a tolerable range, and QUICK can be scalable.

5.8 Throughput Fairness

In this micro-benchmark, we evaluate the fairness control component of QUICK. We run 400 rounds of downlink transmissions for each network with identical transmitting power. In Fig. 18(a), we present the throughput proportion of each user. It is remarkable that the throughput variances of both 802.11ac protocol and QUICK with fairness control are much less than QUICK without fairness control, as shown in both 18(a) and (b). That means the fairness control mechanism we proposed works effectively. Furthermore, as shown in 18(b), both QUICK with/without fairness control, can improve per-user throughput significantly (about 15Mbps) due to CSI feedback overhead saving. Meanwhile, fairness control mechanism causes almost no throughput loss compared

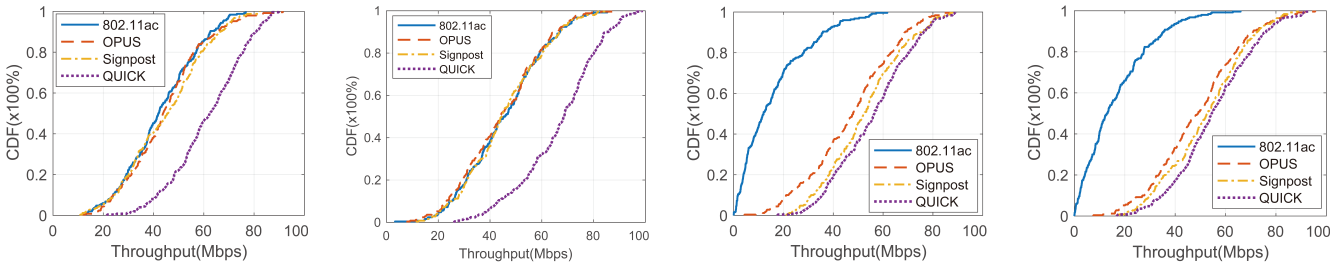

(a) Mobile in downlink (b) Static in downlink (c) Mobile in uplink (d) Static in uplink

Figure 16. The throughput comparison *under accurate CSI*

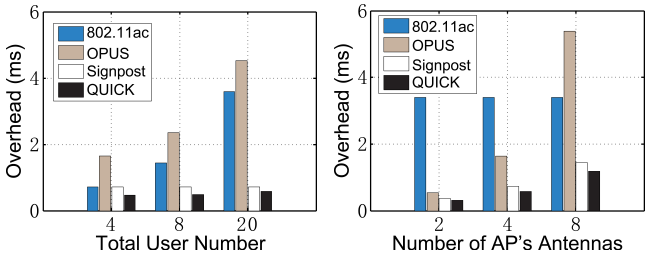

Figure 17. CSI feedback overhead analysis.

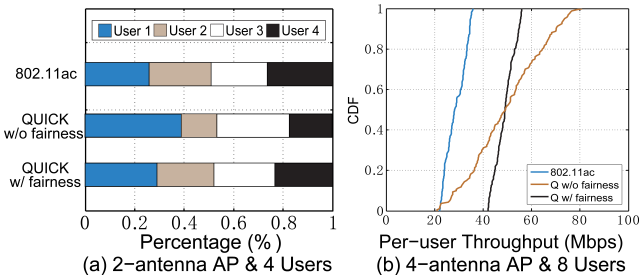

Figure 18. Effectiveness of fairness control mechanism.

to QUICK without fairness control (*i.e.*, selecting users according to the orthogonality among all users). That is because that: (i) The fairness control does not incur MAC-layer overhead. (ii) The CML-based user scheduling can also ensure the selected users to be orthogonal.

6 Conclusion

Our work demonstrates that the inaccurate and unnecessary CSI feedback from concurrent users will lower the throughput in MU-MIMO network. Due to the invalid data transmission and high additional overhead, much consequential superfluous energy consumption and potential channel collision will largely increase the burden of battery limited EWS, which narrow its applications in IoT scenario. Hence, we propose QUICK to improve CSI accuracy and reduce unnecessary CSI feedback for MU-MIMO WLANs. We design an enhanced channel estimation mechanism to calibrate the incorrect CSI measurement and a method to determine whether a CSI report is necessary, which significantly improve channel throughput. We implement the prototype QUICK over software-radio devices. Extensive experiment results show that QUICK can substantially improve the throughput for MU-MIMO networks.

7 Acknowledgments

We sincerely thank our shepherd, Prof. Utz Roedig, and the anonymous reviewers for their insightful comments and suggestions. This work was partially supported by National Key R&D Program of China 2017YFB1003000, NSFC Grant No. 61751211, 61772413, 61672424.

8 References

[1] N. Anand, R. E. Guerra, and E. W. Knightly. The case for UHF-band MU-MIMO. In *Proceedings of ACM MobiCom*, pages 29–40, 2014.

[2] I. E. Bagci, U. Roedig, I. Martinovic, M. Schulz, and M. Hollick. Using channel state information for tamper detection in the internet of things. In *Computer Security Applications Conference*, pages 131–140, 2015.

[3] M. Bor, A. King, and U. Roedig. Lifetime bounds of wi-fi enabled sensor nodes. *Procedia Computer Science*, 52(1):1108–1113, 2015.

[4] Y. Cai, W. Xi, Z. Wang, K. Zhao, J. Han, C. Qian, H. Ding, and J. Zhao. Csi feedback reduction by checking its validity period: poster. In *International Conference on Mobile Computing and NETWORKING*, pages 469–470, 2016.

[5] R. Crepaldi, J. Lee, R. Etkin, and S. J. Lee. Csi-sf: Estimating wireless channel state using csi sampling & fusion. In *IEEE INFOCOM*, pages 154–162, 2012.

[6] A. Das and B. D. Rao. SNR and Noise Variance Estimation for MIMO Systems. *IEEE Transactions on Signal Processing*, 60(60):3929–3941, 2012.

[7] L. Deek, E. Garcia-Villegas, E. Belding, S.-J. Lee, and K. Almeroth. Joint rate and channel width adaptation for 802.11 MIMO wireless networks. In *Proceedings of IEEE SECON*, pages 167–175, 2013.

[8] M. Gast. *802.11ac: A Survival Guide*. O'Reilly Media, 2013.

[9] E. Gelal, J. Ning, K. Pelechrinis, T.-S. Kim, I. Broustis, S. V. Krishnamurthy, and B. D. Rao. Topology control for effective interference cancellation in multiuser mimo networks. *IEEE/ACM Transactions on Networking*, 21(2):455–468, 2013.

[10] D. Halperin, W. Hu, A. Sheth, and D. Wetherall. Tool release:gathering 802.11n traces with channel state information. *Acm Sigcomm Computer Communication Review*, 41(1):53–53, 2011.

[11] C. Husmann, G. Georgis, K. Nikitopoulos, K. Jamieson, J. Zhou, B. Congdon, J. Xiong, K. Sundaresan, K. Jamieson, A. Khojastepour, et al. Flexcore: Massively parallel and flexible processing for large mimo access points. In *Proceedings of USENIX NSDI 17*.

[12] Z.-P. Jiang, W. Xi, X. Li, S. Tang, J.-Z. Zhao, J.-S. Han, K. Zhao, Z. Wang, and B. Xiao. Communicating is crowdsourcing: Wi-fi indoor localization with csi-based speed estimation. *Journal of Computer Science and Technology*, 29(4):589–604, 2014.

[13] M. O. Khan, L. Qiu, A. Bhartia, and K. C.-J. Lin. Smart retransmission and rate adaptation in WiFi. In *Proceedings of IEEE ICNP*, 2015.

[14] S. Li, S. Sen, and D. Koutsonikolas. Bringing mobility-awareness to wlans using phy layer information. pages 53–66, 2014.

[15] R. Liao, B. Bellalta, M. Oliver, and Z. Niu. MU-MIMO MAC protocols for wireless local area networks: A survey. *IEEE Communications Surveys & Tutorials*, 18(1):162–183, 2016.

[16] Y. Ma, G. Zhou, S. Lin, and H. Chen. Rofi: Rotation-aware wifi channel feedback. *IEEE Internet of Things Journal*, PP(99):1–1, 2017.

[17] E. Perahia and R. Stacey. *Next Generation Wireless LANs: 802.11n and 802.11ac*. Cambridge University Press, 2013.

[18] J. G. Proakis and M. Salehi. *Digital communications*. McGraw-Hill Education, 2007.

[19] L. Ravindranath, C. Newport, H. Balakrishnan, and S. Madden. Improving wireless network performance using sensor hints. In *Usenix Conference on Networked Systems Design and Implementation*, pages 281–294, 2011.

[20] L. Shangguan, Z. Yang, A. X. Liu, Z. Zhou, and Y. Liu. Stpp: Spatial-temporal phase profiling-based method for relative rfid tag localization. *IEEE/ACM Transactions on Networking*, 25(1):596–609, 2017.

[21] C. Shepard, A. Javed, and L. Zhong. Control channel design for many-antenna MU-MIMO. In *Proceedings of ACM MobiCom*, pages 578–591, 2015.

[22] S. Sur, I. Pefkianakis, X. Zhang, and K.-H. Kim. Practical mu-mimo user selection on 802.11 ac commodity networks. In *Proceedings of ACM MobiCom*, pages 122–134. ACM, 2016.

[23] Y. C. Tung, S. Han, D. Chen, and K. G. Shin. Vulnerability and protection of channel state information in multiuser mimo networks. 22(3):775–786, 2014.

[24] K. Wu, J. Xiao, Y. Yi, D. Chen, X. Luo, and L. M. Ni. Csi-based indoor localization. *IEEE Transactions on Parallel & Distributed Systems*, 24(7):1300–1309, 2013.

[25] W. Xi, R. Ma, Y. Cai, and K. Zhao. Prevent csi spoofing in uplink mu-mimo transmission. In *The Workshop on Context Sensing & Activity Recognition*, pages 13–18, 2015.

[26] J. Xiao, K. Wu, Y. Yi, L. Wang, and L. M. Ni. Fimd: Fine-grained device-free motion detection. 90(1):229–235, 2012.

[27] X. Xie, E. Chai, X. Zhang, K. Sundaresan, A. Khojastepour, and S. Rangarajan. Hekaton: Efficient and practical large-scale MIMO. In *Proceedings of ACM MobiCom*, pages 304–316, 2015.

[28] X. Xie and X. Zhang. Scalable user selection for MU-MIMO networks. In *Proceedings of IEEE INFOCOM*, 2014.

[29] X. Xie, X. Zhang, and K. Sundaresan. Adaptive feedback compression for mimo networks. In *International Conference on Mobile Computing & NETWORKING*, pages 477–488, 2013.

[30] T. Yoo and A. Goldsmith. On the optimality of multiantenna broadcast scheduling using zero-forcing beamforming. *IEEE Journal on Selected Areas in Communications*, 24(3):528–541, 2006.

[31] X. Zheng, J. Wang, L. Shangguan, Z. Zhou, and Y. Liu. Smokey: Ubiquitous smoking detection with commercial wifi infrastructures. In *IEEE INFOCOM 2016 - the IEEE International Conference on Computer Communications*, pages 1–9, 2016.

[32] X. Zheng, J. Wang, L. Shangguan, Z. Zhou, and Y. Liu. Design and implementation of a csi-based ubiquitous smoking detection system. *IEEE/ACM Transactions on Networking*, PP(99):1–13, 2017.

[33] A. Zhou, T. Wei, X. Zhang, M. Liu, and Z. Li. Signpost:scalable mu-mimo signaling with zero csi feedback. pages 327–336, 2015.